JOURNAL OF GEOPHYSICAL RESEARCH, VOL. 114, A08210, doi:10.1029/2008JA013873, 2009

THEMIS observations of extreme magnetopause motion caused by a hot flow anomaly

K. S. Jacobsen,[1] T. D. Phan,[2] J. P. Eastwood,[2] D. G. Sibeck,[3] J. I. Moen,[1] V. Angelopoulos,[4] J. P. McFadden,[2] M. J. Engebretson,[5] G. Provan,[6] D. Larson,[2] and K.-H. Fornaçon[7]

Received 4 November 2008; revised 18 May 2009; accepted 29 May 2009; published 18 August 2009.

[1] On 30 October 2007, the five THEMIS spacecraft observed the cause and consequence of extreme motion of the dawn flank magnetopause, displacing the magnetopause outward by at least 4.8 R_E in 59 s, with flow speeds in the direction normal to the model magnetopause reaching 800 km/s. While the THEMIS A, C, D, and E observations allowed the determination of the velocity, size, and shape of a large bulge moving tailward along the magnetopause at a speed of 355 km/s, THEMIS B observed the signatures of a hot flow anomaly (HFA) upstream of the bow shock at the same time, indicating that the pressure perturbation generated by the HFA may be the source of the fast compression and expansion of the magnetosphere. The transient deformation of the magnetopause generated field-aligned currents and created traveling convection vortices which were detected by ground magnetometers. This event demonstrates that kinetic (non-MHD) effects at the bow shock can have global consequences on the magnetosphere.

Citation: Jacobsen, K. S., et al. (2009), THEMIS observations of extreme magnetopause motion caused by a hot flow anomaly, *J. Geophys. Res.*, *114*, A08210, doi:10.1029/2008JA013873.

1. Introduction

[2] It is well known that the magnetopause moves and changes in response to varying solar wind conditions. Several studies have been conducted to determine the typical thickness and speed of the magnetopause for different solar wind conditions [e.g., *Berchem and Russell*, 1982; *Le and Russell*, 1994; *Paschmann et al.*, 1993]. *Phan and Paschmann* [1996] found average velocities of the magnetopause in the direction normal to the magnetopause to be 40 km/s or less, with a maximum recorded value of 162 km/s. *Winterhalter et al.* [1981] also observed a magnetopause speed of 195 km/s, and *Sibeck* [1995] reported a speed of 300 km/s. The most obvious cause of this kind of motion is pressure variation in the solar wind, but it can also result from nonlinear interaction in the boundary layers upstream of the Earth's magnetosphere.

[3] In particular, a discontinuity in the solar wind magnetic field hitting the bow shock will for certain field configurations cause a violent reaction, known as a hot flow anomaly (HFA), that creates strong density variations, plasma heating and flow deflections. As the disturbance propagates downstream, it will cause magnetopause motion. More information about HFAs is presented in section 2.

[4] Transient magnetopause deformations can cause ground signatures as they move tailward, as described by *Glassmeier* [1992] and *Kataoka et al.* [2002]. Deformations of the magnetopause cause field-aligned currents that in turn create Traveling Convection Vortices (TCV), which are detected as Magnetic Impulse Events (MIE) by magnetometers on the ground.

[5] The observations presented in this paper show magnetopause motion of large amplitude and a much greater speed than previously seen. Through multispacecraft observations we are able to infer the shape of the deformed magnetopause. Observations of the pristine solar wind by ACE and the solar wind just upstream of the dawn bow shock by THEMIS B reveal the cause for the drastic magnetopause motion, and ground observations provide complementary information on the deformation of the magnetopause.

2. Hot Flow Anomalies

[6] HFAs were first discovered in the mid-1980s, in association with the passage of interplanetary current sheets [*Schwartz et al.*, 1985; *Thomsen et al.*, 1986] A number of simulations were performed, exploring different theoretical explanations for the phenomenon. *Burgess and Schwartz* [1988] found that a magnetic field reversal convecting into a shock led to overreflection followed by upstream penetration of ions from the shock. The reflected ions are thermal-

[1]Department of Physics, University of Oslo, Oslo, Norway.
[2]Space Sciences Laboratory, University of California, Berkeley, California, USA.
[3]NASA Goddard Space Flight Center, Greenbelt, Maryland, USA.
[4]IGPP, ESS, University of California, Los Angeles, California, USA.
[5]Department of Physics, Augsburg College, Minneapolis, Minnesota, USA.
[6]Department of Physics and Astronomy, University of Leicester, Leicester, UK.
[7]IGEP, Technische Universität Braunschweig, Braunschweig, Germany.

0148-0227/09/2008JA013873$09.00

ized through ion beam instabilities. *Burgess* [1989] investigated the role of the convection electric field ($-\mathbf{V} \times \mathbf{B}$) and found that a convection electric field pointing toward the discontinuity is necessary to focus the reflected ions into the discontinuity. *Thomsen et al.* [1993] provided an observational test of the importance of the convection electric field, which confirmed the results of the simulations by Burgess.

[7] *Schwartz* [1995] reviewed the current knowledge of HFAs and summarized the observational characteristics, of which the main points were as follows:

[8] 1. The events are flanked by regions of enhanced magnetic field strength, plasma density, and a slight increase in temperature. Sometimes only one edge shows these characteristics.

[9] 2. The central regions of HFAs contain hot (10^6–10^7 K) plasma that is flowing significantly slower than the ambient solar wind and is highly deflected from the Sun-Earth line. The magnetic field drops, and the density is at or below solar wind values.

[10] 3. HFAs are found associated with gross changes in the IMF direction.

[11] 4. HFAs convect with the solar wind flow.

[12] Interest in HFAs was renewed in the late 1990s, as observations were made of a large magnetopause deformation associated with a HFA [*Sibeck et al.*, 1998, 1999]. They found an outward movement of 5 Earth radii (R_E) in 7 min resulting from a HFA. *Schwartz et al.* [2000] performed a study of 30 HFAs, and amongst other results, calculated an occurrence rate of 3 per day. These results indicate that HFAs are more common and have a far greater influence on the magnetosphere than previously thought. *Sibeck et al.* [2000] further investigated HFAs, and a short summary of their conceptual HFA model can be seen in Figure 1 of that paper.

[13] The most recent theoretical work on HFAs is a hybrid simulation by *Lin* [2002], in which she studied the formation and structure of strong HFAs at the bow shock and in the magnetosheath, and their effects on the magnetopause. A statistical study of HFAs using data from the Cluster mission confirmed some of the predictions from that simulation, and presented evidence that fast solar wind is an essential condition for HFA formation [*Facsko et al.*, 2008].

[14] *Eastwood et al.* [2008] observed a HFA both up and downstream of the bow shock simultaneously. They noted that the resulting pressure perturbation would cause a significant shift in the magnetopause location but no direct observations of the magnetopause were available in that event.

[15] To summarize, a HFA is generated when a discontinuity in the solar wind magnetic field hits the bow shock under certain conditions. The most important condition is that the convection electric field points toward the discontinuity on at least one side. Ions reflected from the bow shock are focused into the discontinuity, where they thermalize through ion beam instabilities. This causes plasma pressure to rise, which in turn leads to an expansion of the heated plasma into the ambient plasmas both upstream and downstream of the bow shock. This expansion leads to a drop in density and magnetic field strength, and may compress plasma and magnetic field on one or both sides of the expanded area. It also causes a change in the local plasma flow, which may even become sunward in some cases. This structure is what is detected as a HFA. A strong HFA will propagate through the magnetosheath and hit the magnetopause, at which point the variations in ram pressure will cause the magnetosphere to compress or expand as the regions of enhanced and depleted density arrive.

3. Orbits and Instrumentation

[16] On 30 October 2007 THEMIS [*Angelopoulos*, 2008] was in the orbit placement stage of its mission, and the spacecraft were approximately aligned along the GSM Y axis with smaller differences in X and Z. As shown in Figure 1, THEMIS A, D and E were just inside the magnetosphere, C was in the magnetosheath, and B was in the solar wind. All spacecraft were moving at less than 2 km/s, which is negligible for the phenomenon described in this paper. Data from the fluxgate magnetometer (FGM) [*Auster et al.*, 2008] and the electrostatic plasma analyzer (ESA) [*McFadden et al.*, 2008] are used. For the solar wind observations, the THEMIS B ESA was in the 32 energy sweeps/spin mode, which does not fully resolve the narrow solar wind beam. Thus the absolute values of the solar wind ion moments and their variations should be considered qualitative.

4. Observations

4.1. Magnetopause Observations

[17] Figure 2 shows data from the magnetic field experiment (FGM) and the thermal plasma instrument (ESA) for THEMIS A, C, D and E. At 1404:55 UT, THEMIS D entered the magnetosheath. It remained in the magnetosheath until 1406:20 UT, and immediately after exiting it, a velocity of 800 km/s normal to the model magnetopause [*Fairfield*, 1971] was observed. This is much larger than previously reported values for magnetopause motion.

[18] To place this observation in context, the order of the spacecraft shown in Figure 2 is sorted by the spacecraft distance from the model magnetopause. THEMIS C was in the magnetosheath, the rest were inside the magnetopause. A was the closest spacecraft to the model magnetopause, followed by D, then E. Spacecraft A, D and E all had brief encounters with the magnetosheath, but not in the order of proximity to the magnetopause, which means that this was not a one-dimensional large-scale compression of the magnetosphere. Instead, entry into the magnetosheath was ordered by position in X_{GSE}. Spacecraft D entered first, followed in succession by E and A, located further down the flank. This suggests that there was an inward deformation of the magnetopause which progressed tailward. Assuming that this is true, and that the large-scale shape of the inward bulge did not change much as it passed by A, D and E, we can estimate its velocity along the magnetopause. We use the middle of the magnetosheath encounters for these calculations, as the bulge width decreases with increasing distance from the magnetopause, but the center should remain approximately the same. Dividing the distance tailward along the model magnetopause from one magnetosheath encounter to another by the time difference, we obtain the values shown in Table 1. The speed of the bulge is remarkably similar for the 3 spacecraft pairs, with an average of 355 km/s. Multiplying the velocity by the

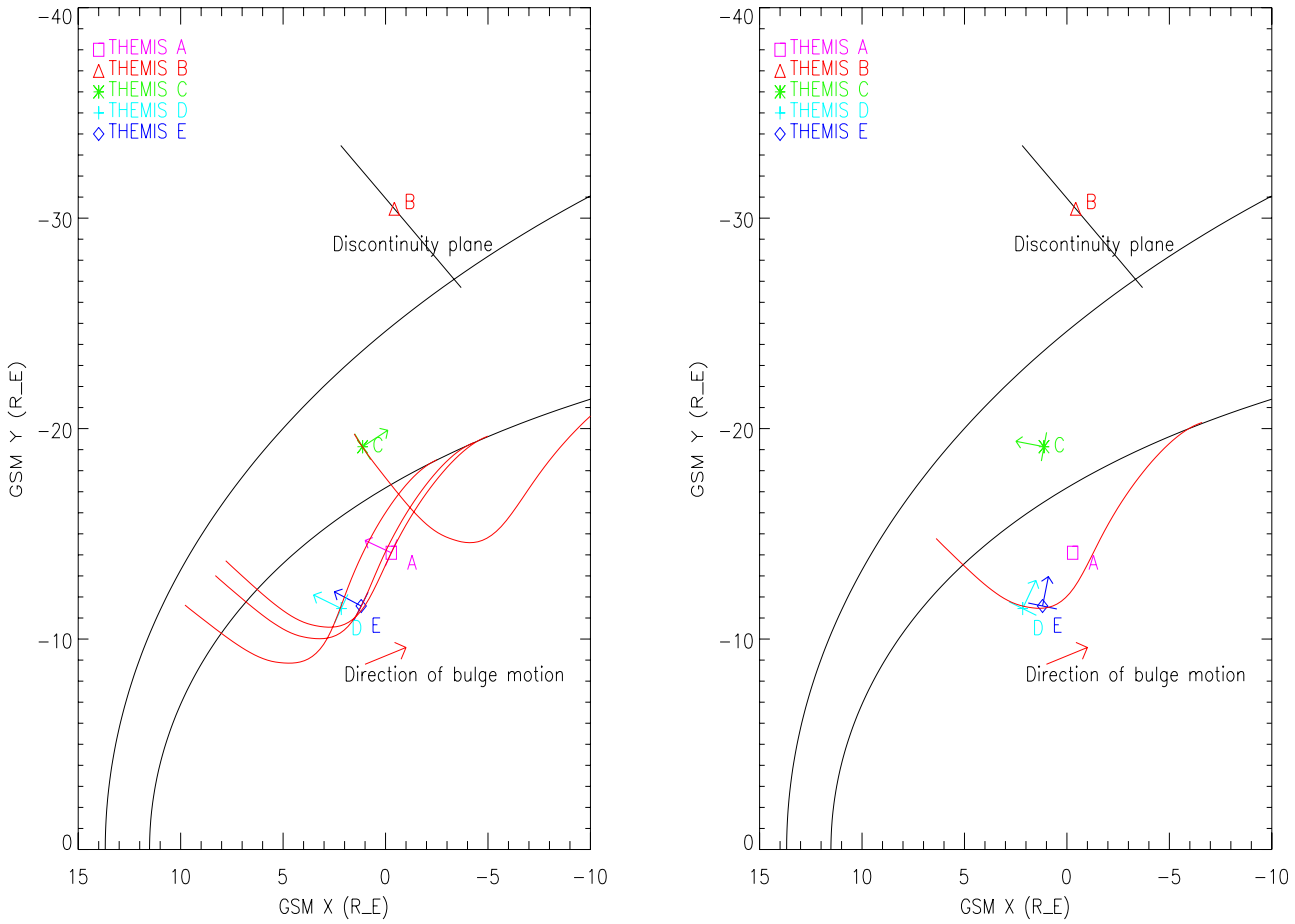

Figure 1. (left) Magnetopause [*Shue et al.*, 1997], bow shock [*Farris et al.*, 1991; *Cairns et al.*, 1995], positions of the THEMIS spacecraft, and the orientation of the discontinuity plane in the solar wind are shown, together with normals for the first magnetopause crossing for each of the spacecraft, and drawings of the magnetopause bulge. (right) The same as Figure 1 (left), but normals for each spacecraft's second magnetopause crossing are shown together with the inferred magnetopause.

magnetosheath encounter durations, we obtain a measure of the width of the bulge along the model magnetopause at different distances to the model magnetopause. The width of the bulge is 6.1 R_E for A, 4.7 R_E for D, and 2.8 R_E for E.

[19] At 1407:30 UT THEMIS A entered the magnetosphere and at 1408:35 UT the magnetic field observations of THEMIS C indicate that it also entered the magnetosphere. The spacecraft were separated by 4.77 R_E in the normal direction but only 0.32 R_E tailward along the model magnetopause. This separation makes them well suited to get an estimate for the amplitude and speed of the magnetopause in the direction normal to the model magnetopause. Using the estimated velocity of the bulge tailward, we subtract 6 s from the time interval to account for the distance along the model magnetopause. The magnetopause moved outward at least 4.77 R_E in less than 59 s, which gives an average velocity normal to the model magnetopause of at least 515 km/s for this time interval. This agrees with the plasma measurements, which detected velocities normal to the model magnetopause of approximately 300, 800 and 600 km/s for THEMIS A, D and E (Figures 2c, 2f, and 2i).

[20] Performing the minimum variance analysis (MVA) [*Sonnerup and Cahill*, 1967] on the magnetic field data of each spacecraft for each crossing into and out of the magnetosheath, we find the normals of the actual magnetopause. For THEMIS A, D and E, the normals for the first crossings are all well defined, with intermediate-to-minimum eigenvalue ratios greater than 10. The rest of the normals are reasonably well defined, with eigenvalue ratios of at least 4. The magnetic field sampling frequency was $\frac{1}{3}$ Hz for THEMIS C, and 4 Hz for the other spacecraft. The results of MVA may vary with the length of the time interval chosen for analysis. If the results vary greatly for different time intervals, they are unreliable. Because of this, intervals with lengths ranging from 10 to 120 s were examined. The time intervals used for the final values range from 20 to 35 s for the different spacecraft. The normal for the second crossing of THEMIS A changes significantly when using different time intervals for the MVA analysis, which indicates that it cannot be trusted.

[21] Using these normals and the estimated values above, we reconstruct the shape of the bulge on the magnetopause. The result is seen in Figure 1. On the left the MVA normals for the first crossings are shown together with drawings of the bulge, and the normals for the second crossings are shown on the right. THEMIS A, D and E first crossed the magnetopause going from the magnetosphere to the mag-

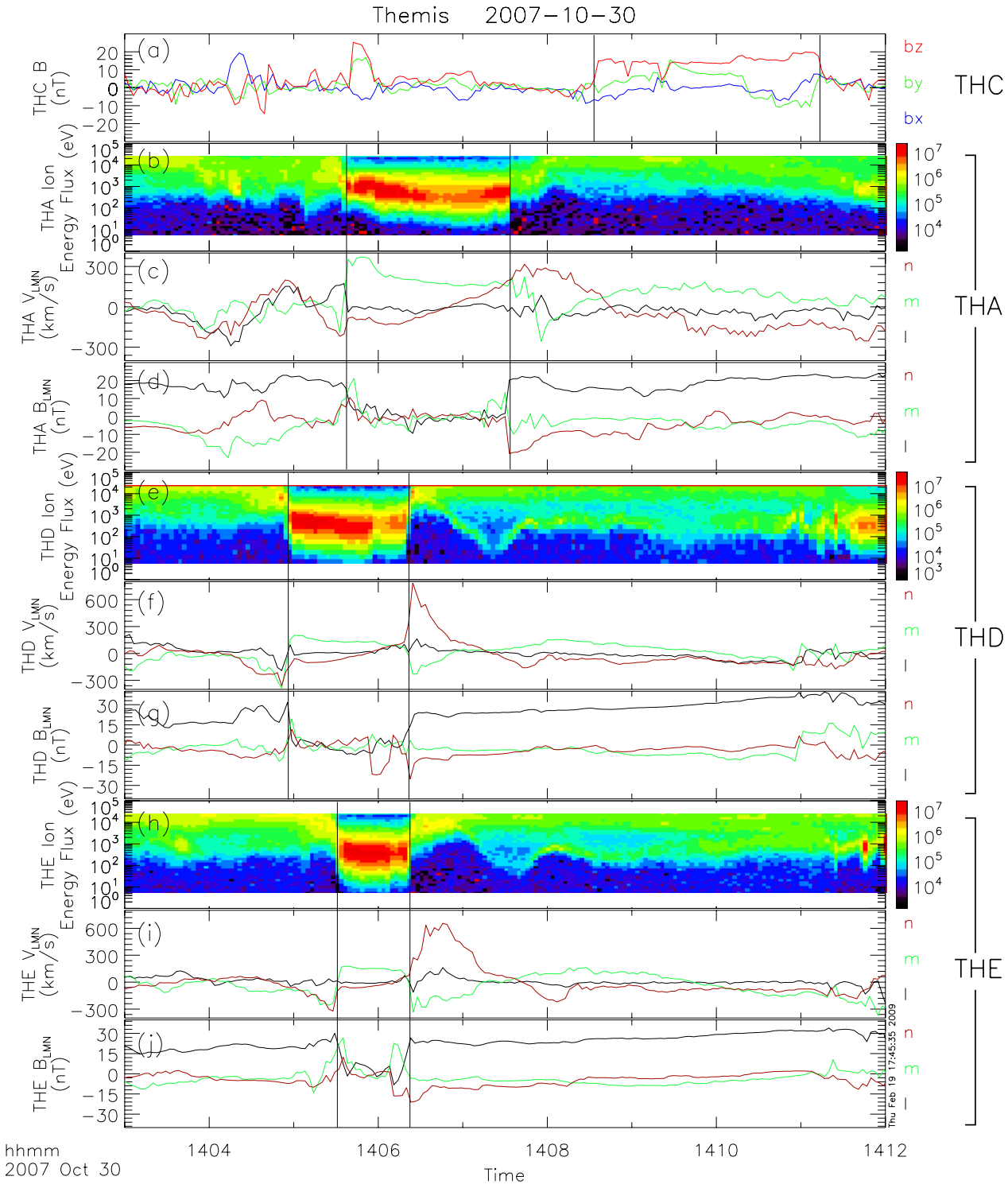

Figure 2. THEMIS A, C, D, and E data. (a) THEMIS C magnetic field. (b–d) THEMIS A ion energy flux spectrogram, velocity, and magnetic field. (e–g) Same for THEMIS D. (h–j) Same for THEMIS E. The velocity and magnetic field for THEMIS A, D, and E are plotted in the LMN coordinate system, using the average magnetopause normal of *Fairfield* [1971], where M is eastward along the model magnetopause, N is normal to the model magnetopause, and L completes the right-handed, orthogonal system. The unit of the spectrograms is eV s^{-1} cm^{-2} sr^{-1} eV^{-1}. The spacecraft are sorted by distance from the model magnetopause, with THEMIS C being in the magnetosheath and the rest being in the magnetosphere. Of the spacecraft in the magnetosphere, THEMIS A is the closest to the model magnetopause. THEMIS A, D, and E have brief encounters with the magnetosheath and THEMIS C encounters the magnetosphere, indicating large-scale magnetopause motion. Magnetopause crossings are indicated by vertical lines.

Table 1. Magnetopause Bulge Speed Along the Model Magnetopause

Spacecraft Used in Calculation	Speed (km/s)
D and E	359
D and A	354
E and A	352

netosheath, and then again as they left the magnetosheath and entered the magnetosphere. For THEMIS C, starting in the magnetosheath, the first crossing was from the magnetosheath to the magnetosphere and the second was from the magnetosphere to the magnetosheath. The shape is drawn to best fit the normals and estimated values. It has been rotated and translated to line up with the different spacecraft while its front end is still attached to the magnetopause. The shape of the magnetopause deformation after the entry of THEMIS C into the magnetosphere is less certain, and has not been drawn. THEMIS C spent 160 s in the magnetosphere, longer than any of the other spacecraft spent in the magnetosheath, which indicates that the outward bulge is larger than the inward bulge.

[22] Just before 1406 UT, THEMIS C had a short encounter with a magnetic field resembling that of the magnetosphere. The timing of the encounter in relation to the timing of magnetopause crossings by the other spacecraft, and the normal vectors resulting from MVA performed on the magnetic field data, was analyzed. For this to be an actual magnetosphere encounter would require a very unusual magnetopause structure and a magnetopause motion at a speed of several thousand km/s. The observed location and timing of the crossings, and the corresponding crossing normals, are better explained by a crossing of the earthward side of a detached flux rope moving antisunward. Unfortunately, there are no particle data from THEMIS C at this time, and the magnetic field data are limited to spin resolution. This makes it difficult to have a positive identification either way.

4.2. Ground Observations

[23] A large, transient magnetopause deformation should have ground signatures. Specifically, one should expect two or more convection vortices to travel from the dayside to the nightside [*Sibeck et al.*, 2003; *Kataoka et al.*, 2004]. A compression followed by an expansion of the magnetosphere is expected to produce a clockwise vortex followed by a counterclockwise vortex.

[24] Figure 3 shows two subsequent SuperDARN [*Greenwald et al.*, 1995; *Chisham et al.*, 2007] convection maps taken at 1406 UT and 1408 UT. In the first we see a counterclockwise vortex, and in the second a clockwise vortex. Although there is some lack of backscatter to constrain the map-potential algorithm, especially on the equatorward edge of the flow vortex at 1406 UT, the observation of these flow vortices in conjunction with the HFA observed by THEMIS B is remarkable. The SuperDARN data do not in actuality show the speed and direction in which the vortices were traveling, as each vortex was detected in only one convection map.

[25] In data from the THEMIS magnetometer array [*Russell et al.*, 2008; *Mende et al.*, 2008; *Glassmeier et al.*, 2008], shown in Figure 4, a magnetic impulse event (MIE) is seen by several magnetometers. The main characteristic of the MIE is a positive peak in the X component,

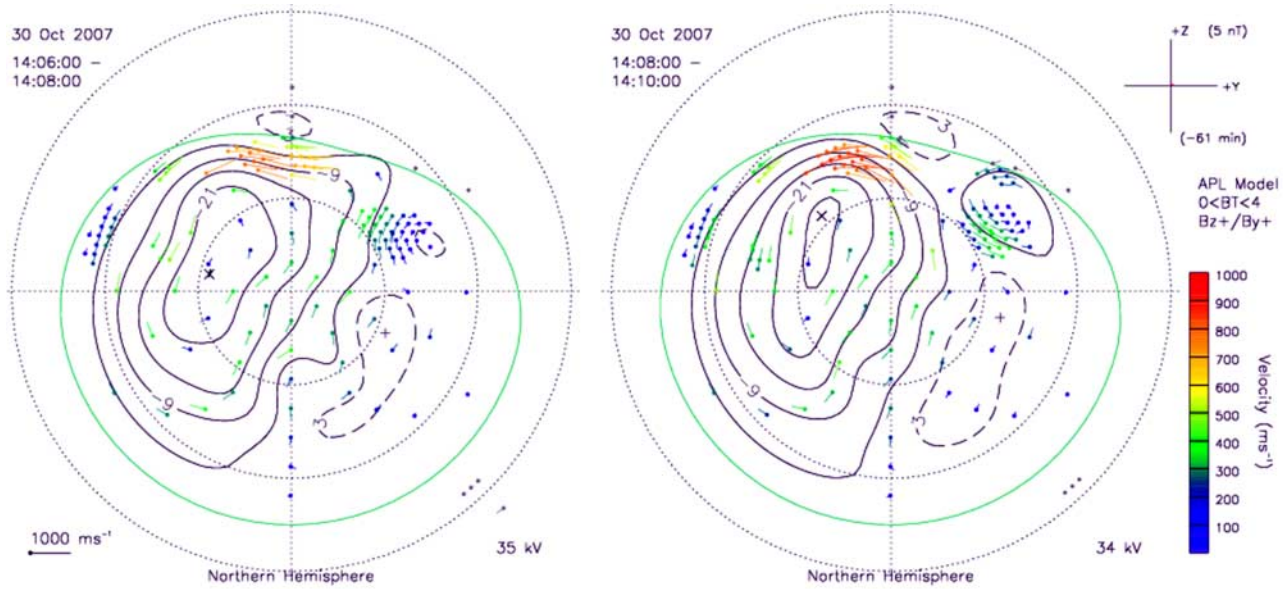

Figure 3. Data from the SuperDARN radar network. Measurements are indicated by dots, with lines pointing out in the direction of the plasma flow. The magnitude of the velocity is indicated by both the length of the line and its color. In areas with no measurements available, the dots and lines are based on a computer model. The black lines are equipotential contours calculated by a computer model, with the cross and plus symbols marking the minimum and maximum values. The green line characterizes the size of the convection zone. SuperDARN observed first a counterclockwise convection vortex, shown on the left, and then a clockwise convection vortex, shown on the right.

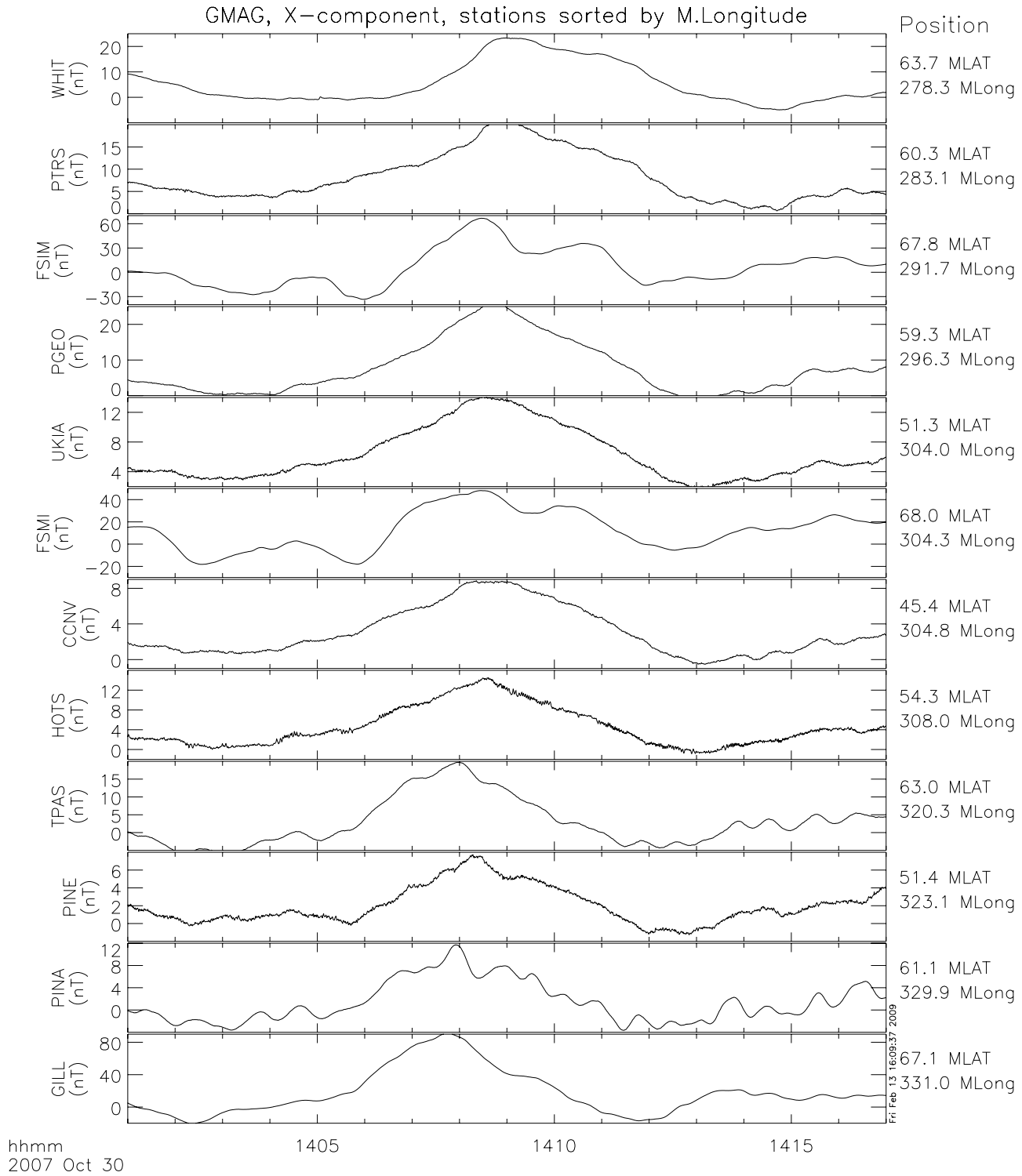

Figure 4. THEMIS ground magnetometer data. Stations are sorted by magnetic longitude from low to high. For each station, the X (north-south) component of the magnetic field is plotted. The long-term average magnetic field has been subtracted. To the right of the plot the positions of the stations in magnetic latitude and longitude are shown. A MIE in the form of a positive peak in the X component is seen moving westward.

which is consistent with a clockwise vortex passing somewhere to the north of the stations. The first station to detect the MIE is GILL, located at 0730 MLT. The central peak of the MIE is seen by GILL at 1407:45 UT, and moves to earlier magnetic local times. WHIT, at 0400 MLT, sees the peak at 1409:05 UT. The ground speed of the MIE is ~25 km/s, going west. The direction is what we expect for a MIE caused by a tailward moving magnetopause deformation at

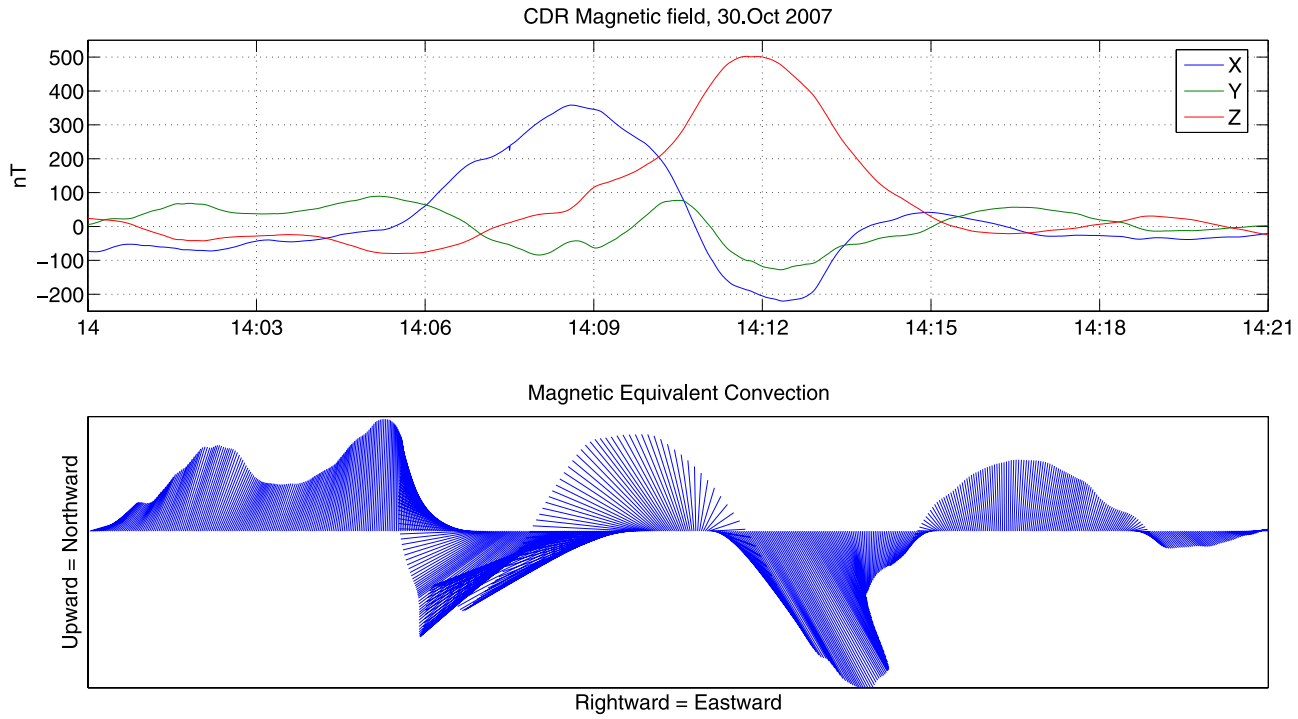

Figure 5. Data from the ground magnetometer station CDR of the MACCS array. (top) Magnetic field disturbance in local geomagnetic coordinates. (bottom) Magnetic equivalent convection (MEC). During the large fluctuations from 1406 to 1415, the MEC is consistent with the passage of a pair of convection vortices.

the dawn flank. We also note that the peak-to-peak amplitude of the MIE tends to be larger at higher latitudes, which is consistent with the convection vortex traveling at a higher latitude than these magnetometers.

[26] At 1408 UT the magnetometer station at Cape Dorset, which is part of the MACCS array [*Hughes and Engebretson*, 1997], was located at 0913 MLT and 73.5 Magnetic latitude, which is very close to the path we expect the vortices to travel. Figure 5 shows data from this station. Between 1406 and 1415 UT, a large magnetic field perturbation is seen, with peak-to-peak amplitudes of 200 nT for By and more than 500 nT for Bx and Bz. Figure 5 (bottom) shows the Magnetic Equivalent Convection (MEC). MEC can be used as an approximation to the plasma convection when the magnetic disturbance is caused mainly by ionospheric Hall currents. Assuming this to be the case for the interval 1406 to 1415, we see signatures consistent with a counterclockwise vortex followed by a clockwise vortex passing westward, with the vortex centers at a latitude south of the station.

[27] Although convection vortices were observed around the same time as the magnetopause deformations, and moving in the expected way, they were not ordered as expected. Either the compression did not cause a vortex, the ground instrumentation missed a vortex, or our understanding is incomplete. In any case, this shows that the HFA ultimately led to disturbances in the ionosphere.

4.3. ACE and THEMIS B Observations in the Solar Wind

[28] To investigate the cause for the large amplitude perturbation on the magnetopause we examine the upstream solar wind measurements. During this event, the Advanced Composition Explorer (ACE) was at L1 in the pristine solar wind while THEMIS B was in the solar wind just upstream of the dawn bow shock (Figure 1). There were no changes in the solar wind plasma parameters (Figures 6f–6l) measured by ACE that could account for rapid motion of the magnetopause.

[29] Figure 6 shows data from ACE and THEMIS B. Comparing the magnetic field of ACE, located far upstream, to the magnetic field of THEMIS B, located just upstream of the dawn bow shock, we find the drop in B_Z, which is much sharper now, at 1404:40 UT. Following this drop, a small population of high-energy ions is detected. These are ions reflected from the bow shock, to which THEMIS B is now magnetically connected.

[30] At 1406:40 UT, THEMIS B detected something which was not present in the ACE data; an interval of disturbed magnetic field with enhanced ion energy flux between 2–10 keV. There was a flow deflection of many tens of km/s, a drop in the density and a temperature increase, resulting in a drop of the dynamic pressure. These are characteristics of a hot flow anomaly (HFA) [*Schwartz et al.*, 1985; *Thomsen et al.*, 1986].

[31] At this time there was also a change in the magnetic field orientation. The reason that this change caused a HFA, while the much larger change in Bz at 1404:40 UT did not, is the criterion for a HFA that the motional electric field must point toward the discontinuity on at least one side [*Thomsen et al.*, 1993]. Using MVA, the normal to the first discontinuity plane is $(0.91,0.39,0.18)_{GSM}$, with an eigenvalue ratio of 7.5. We calculate the convection E field from $\mathbf{E} = -\mathbf{v} \times \mathbf{B}$, and find that the first discontinuity has an

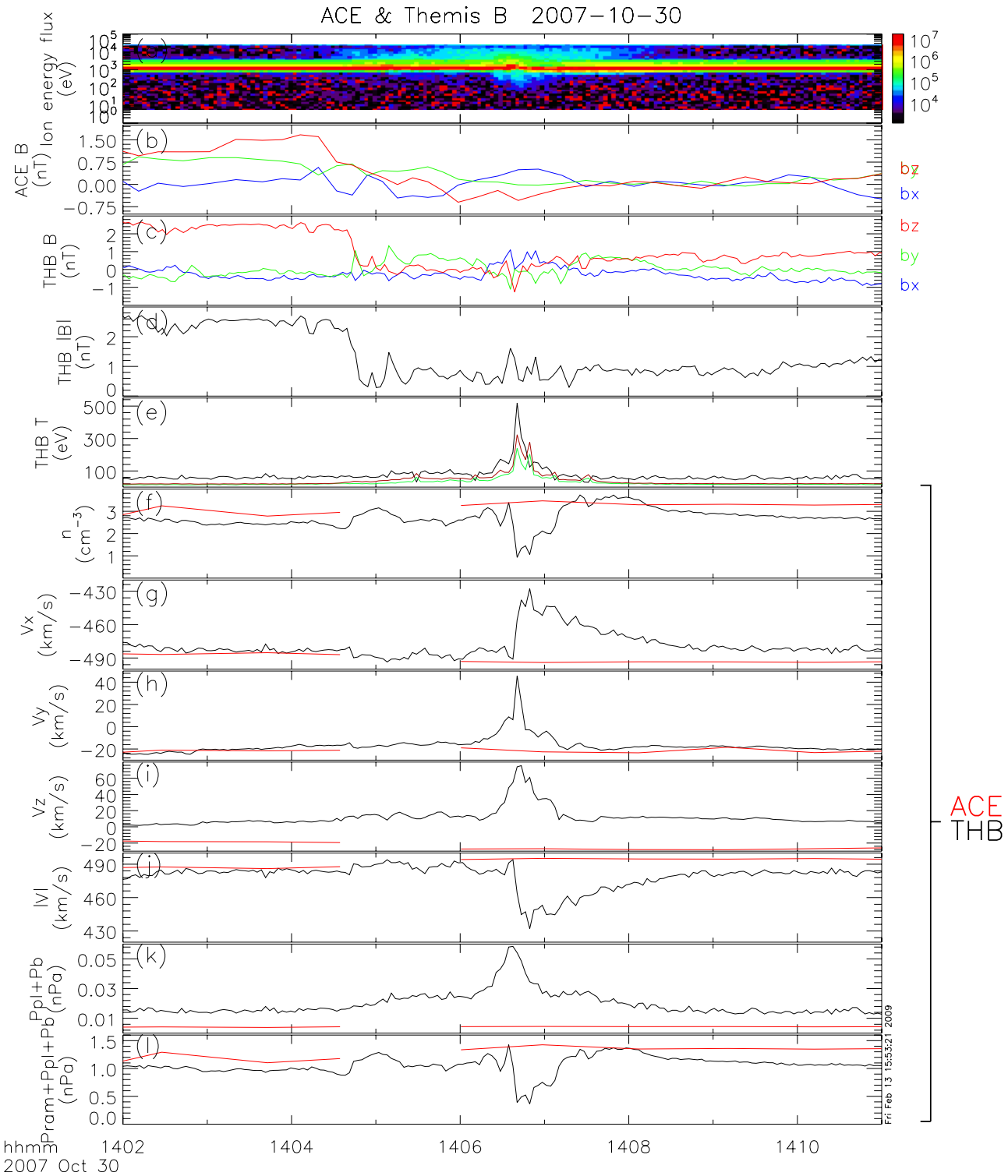

Figure 6. THEMIS B and ACE data. (a) THEMIS B ion energy flux spectrogram (in eV s^{-1} cm^{-2} sr^{-1} eV^{-1}). (b) ACE magnetic field (GSM). (c) THEMIS B magnetic field (GSM). (d) THEMIS B magnetic field magnitude. (e) THEMIS B temperature. (f) Density. (g–j) Velocity GSM X, Y, and Z components and magnitude. (k) Sum of plasma and magnetic pressure. (l) Sum of plasma, magnetic, and ram pressure. In Figures 6f–6l, THEMIS B data are black, and ACE data are red. The ACE data have been time shifted approximately 1 h and 5 min, using first an automatic calculation and then adjusting it according to magnetic signatures close to the time of interest. Around 1406:45, THEMIS B detects magnetic field, density, velocity, and temperature variations consistent with a hot flow anomaly.

electric field pointing away from it on the antisunward side and a very small normal field on the sunward side. The normal to the second discontinuity plane is $(0.75, 0.65, -0.10)_{GSM}$, with an eigenvalue ratio of 3.8. The second discontinuity has a very small normal field on the antisunward side and a field pointing toward it on the sunward side. Thus, only the second discontinuity has an appropriate geometry for HFA formation. The plane of the solar wind discontinuity is shown in Figure 1.

[32] The velocities observed just inside the magnetopause (Figures 2c, 2f, and 2i) are mainly in the N and M directions. This implies that there is no motion of the bulge in the L direction, which points north/south. We interpret this to mean that the bulge is in fact ridge-like, extending north and south. This is consistent with the normal of the discontinuity plane, and the negative M during the outward motion is also consistent with the refilling flow observed in simulation by *Kataoka et al.* [2004].

5. Summary and Conclusions

[33] On 30 October 2007, the five THEMIS spacecraft observed the cause and consequence of extreme motion of the dawn flank magnetopause, with flow speeds in the direction normal to the model magnetopause reaching 800 km/s. Direct observations showed that the magnetopause was displaced outward by at least 4.8 R_E in 59 s. The multispacecraft observations also revealed a bulge on the magnetopause moving tailward at 355 km/s. There was nothing in the solar wind plasma data from ACE that could have caused the magnetopause motion. However, the THEMIS B spacecraft observed the signatures of a hot flow anomaly in the solar wind just upstream of the dawn bow shock, which is likely to be the cause of the fast magnetopause motion.

[34] The following is a summary of our interpretation of the data. On 30 October 2007 a discontinuity in the solar wind magnetic field hit the bow shock. The motional electric field pointed toward the discontinuity on one side, fulfilling an important criterion for HFA generation. The discontinuity swept tailward over the bow shock, with an orientation suited for producing a HFA at the dawn side of the magnetosphere, and THEMIS B did observe signs of a HFA. In the magnetosheath, the HFA created a region of low dynamic pressure surrounded by regions of higher dynamic pressure. As these regions reached the magnetopause, it moved in response to the dynamic pressure variations. As the intersection of the discontinuity with the bow shock moved tailward, so did the HFA structure. The resulting motion of the magnetopause is tailward moving bulges, first inward, then outward. The inward bulge passed over THEMIS A, D and E, allowing us to do a rough reconstruction of its shape. Then, the outward bulge passed THEMIS C, providing direct evidence of rapid, large-amplitude magnetopause motion. The transient deformations of the magnetopause cause field-aligned currents, creating traveling convection vortices which are detected by ground magnetometers.

[35] The multiple spacecraft of the THEMIS mission are clearly a great advantage in the study of events such as these, providing simultaneous measurements from different regions and allowing us to deduce the motion and size of the structures encountered. Our results show that a HFA can have a significant effect on the magnetopause, even when the upstream pristine solar wind was rather unremarkable. This implies that kinetic (non-MHD) effects at the bow shock can have global consequences on the magnetosphere.

[36] We have examined THEMIS data in the period from the start of the mission to June 2008. Though the present event has the highest recorded velocity, there are other events in the THEMIS data set with normal velocities of 400–600 km/s. Further investigation into each event is required to determine if they are also caused by HFAs, and to understand more precisely how the disruption caused by the HFA at the shock is transmitted through the magnetosheath to the magnetosphere.

[37] **Acknowledgments.** We acknowledge the use of data from the Advanced Composition Explorer (ACE). This research was funded by the Research Council of Norway. Most of this work was performed while K. S. Jacobsen was visiting UC Berkeley. This work was supported by NASA grant NAS5-02099 at UC Berkeley. The MACCS array is supported by U.S. National Science Foundation grant ATM-0827903 to Augsburg College. We thank Masaki Fujimoto for his helpful suggestions. The authors thank the referees for their helpful comments.

[38] Zuyin Pu thanks the reviewers for their assistance in evaluating this paper.

References

Angelopoulos, V. (2008), The THEMIS mission, *Space Sci. Rev.*, *141*, 5–43, doi:10.1007/s11214-008-9336-1.

Auster, H. U., et al. (2008), The THEMIS fluxgate magnetometer, *Space Sci. Rev.*, *141*, 235–264, doi:10.1007/s11214-008-9365-9.

Berchem, J., and C. T. Russell (1982), The thickness of the magnetopause current layer: ISEE 1 and 2 observations, *J. Geophys. Res.*, *87*, 2108–2114.

Burgess, D. (1989), On the effect of a tangential discontinuity on ions specularly reflected at an oblique shock, *J. Geophys. Res.*, *94*(A1), 472–478.

Burgess, D., and S. Schwartz (1988), Colliding plasma structures: Current sheet and perpendicular shock, *J. Geophys. Res.*, *93*(A10), 11,327–11,340.

Cairns, I. H., D. H. Fairfield, R. R. Anderson, V. E. H. Carlton, K. I. Paularena, and A. J. Lazarus (1995), Unusual locations of Earth's bow shock on September 24–25, 1987: Mach number effects, *J. Geophys. Res.*, *100*, 47–62.

Chisham, G., et al. (2007), A decade of the Super Dual Auroral Radar Network (SuperDARN): Scientific achievements, new techniques and future directions, *Surv. Geophys.*, *28*, 33–109.

Eastwood, J. P., et al. (2008), THEMIS observations of a hot flow anomaly: Solar wind, magnetosheath, and ground-based measurements, *Geophys. Res. Lett.*, *35*, L17S03, doi:10.1029/2008GL033475.

Facsko, G., K. Kecskemety, G. Erdos, M. Tatrallyay, P. W. Daly, and I. Dandouras (2008), A statistical study of hot flow anomalies using Cluster data, *Adv. Space Res.*, *41*(8), 1286–1291, doi:10.1016/j.asr.2008.02.005.

Fairfield, D. H. (1971), Average and unusual locations of the Earth's magnetopause and bow shock, *J. Geophys. Res.*, *76*, 6700–6716.

Farris, M. H., S. M. Petrinec, and C. T. Russell (1991), The thickness of the magnetosheath: Constraints on the polytropic index, *Geophys. Res. Lett.*, *18*, 1821–1824.

Glassmeier, K. H. (1992), Traveling magnetospheric convection twin-vortices—Observations and theory, *Ann. Geophys.*, *10*, 547–565.

Glassmeier, K.-H., et al. (2008), Magnetospheric quasi-static response to the dynamic magnetosheath: A THEMIS case study, *Geophys. Res. Lett.*, *35*, L17S01, doi:10.1029/2008GL033469.

Greenwald, R. A., et al. (1995), DARN/SuperDARN: A global view of the dynamics of high-latitude convection, *Space Sci. Rev.*, *71*, 761–796.

Hughes, W. J., and M. J. Engebretson (1997), MACCS: Magnetometer Array for Cusp and Cleft Studies, in *Satellite-Ground Based Coordination Sourcebook*, Eur. Space Agency Spec. Publ., *ESA SP-1198*, 119–130.

Kataoka, R., H. Fukunishi, L. J. Lanzerotti, T. J. Rosenberg, A. T. Weatherwax, M. J. Engebretson, and J. Watermann (2002), Traveling convection vortices induced by solar wind tangential discontinuities, *J. Geophys. Res.*, *107*(A12), 1455, doi:10.1029/2002JA009459.

Kataoka, R., H. Fukunishi, S. Fujita, T. Tanaka, and M. Itonaga (2004), Transient response of the Earth's magnetosphere to a localized density pulse in the solar wind: Simulation of traveling convection vortices, *J. Geophys. Res.*, *109*, A03204, doi:10.1029/2003JA010287.

Le, G., and C. T. Russell (1994), The thickness and structure of high beta magnetopause current layer, *Geophys. Res. Lett.*, *21*, 2451–2454.

Lin, Y. (2002), Global hybrid simulation of hot flow anomalies near the bow shock and in the magnetosheath, in *Symposium on Intercomparative Magetosheath Studies, Antalya, Turkey, Sep 04–08, 2000*, *Planet. Space Sci.*, *50*(5–6), 577–591.

McFadden, J. P., C. W. Carlson, D. Larson, M. Ludlam, R. Abiad, B. Elliott, P. Turin, M. Marckwordt, and V. Angelopoulos (2008), The THEMIS ESA Plasma Instrument and in-flight calibration, *Space Sci. Rev.*, *141*, 277–302.

Mende, S. B., S. E. Harris, H. U. Frey, V. Angelopoulos, C. T. Russell, E. Donovan, B. Jackel, M. Greffen, and L. M. Peticolas (2008), The THEMIS array of ground based observatories for the study of auroral substorms, *Space Sci. Rev.*, *141*, 357–387, doi:10.1007/s11214-008-9380.

Paschmann, G., W. Baumjohann, N. Sckopke, T. D. Phan, and H. Lühr (1993), Structure of the dayside magnetopause for low magnetic shear, *J. Geophys. Res.*, *98*, 13,409–13,422.

Phan, T. D., and G. Paschmann (1996), Low-latitude dayside magnetopause and boundary layer for high magnetic shear: 1. Structure and motion, *J. Geophys. Res.*, *101*, 7801–7815.

Russell, C. T., P. J. Chi, D. J. Dearborn, Y. S. Ge, B. Kuo-Tiong, J. D. Means, D. R. Pierce, K. M. Rowe, and R. C. Snare (2008), THEMIS ground-based magnetometers, *Space Sci. Rev.*, *141*, 389–412, doi:10.1007/s11214-008-9337-0.

Schwartz, S. (1995), Hot flow anomalies near the Earth's bow shock, in *Physics of Collisionless Shocks*, edited by C. T. Russell, *Adv. Space Res.*, *15*, 107–116.

Schwartz, S. J., et al. (1985), An active current sheet in the solar wind, *Nature*, *318*, 269–271.

Schwartz, S. J., G. Paschmann, N. Sckopke, T. M. Bauer, M. Dunlop, A. N. Fazakerley, and M. F. Thomsen (2000), Conditions for the formation of hot flow anomalies at Earth's bow shock, *J. Geophys. Res.*, *105*, 12,639–12,650.

Shue, J.-H., J. K. Chao, H. C. Fu, C. T. Russell, P. Song, K. K. Khurana, and H. J. Singer (1997), A new functional form to study the solar wind control of the magnetopause size and shape, *J. Geophys. Res.*, *102*, 9497–9511.

Sibeck, D. G. (1995), The magnetospheric response to foreshock pressure pulses, in *Physics of the Magnetopause*, *Geophys. Monogr. Ser.*, vol. 90, edited by P. Song, B. U. O. Sonnerup, and M. F. Thomsen, pp. 293–302, AGU, Washington, D. C.

Sibeck, D., N. Borodkova, G. Zastenker, S. Romanov, and J. Sauvaud (1998), Gross deformation of the dayside magnetopause, *Geophys. Res. Lett.*, *25*(4), 453–456.

Sibeck, D. G., et al. (1999), Comprehensive study of the magnetospheric response to a hot flow anomaly, *J. Geophy. Res.*, *104*, 4577–4593.

Sibeck, D. G., et al. (2000), Magnetopause motion driven by interplanetary magnetic field variations, *J. Geophys. Res.*, *105*, 25,155–25,169.

Sibeck, D. G., N. B. Trivedi, E. Zesta, R. B. Decker, H. J. Singer, A. Szabo, H. Tachihara, and J. Watermann (2003), Pressure-pulse interaction with the magnetosphere and ionosphere, *J. Geophys. Res.*, *108*(A2), 1095, doi:10.1029/2002JA009675.

Sonnerup, B. U., and L. J. Cahill (1967), Magnetopause structure and attitude from Explorer 12 observations, *J. Geophys. Res.*, *72*, 171–183.

Thomsen, M. F., J. T. Gosling, S. A. Fuselier, S. J. Bame, and C. T. Russell (1986), Hot, diamagnetic cavities upstream from the Earth's bow shock, *J. Geophys. Res.*, *91*, 2961–2973.

Thomsen, M. F., V. A. Thomas, D. Winske, J. T. Gosling, M. H. Farris, and C. T. Russell (1993), Observational test of hot flow anomaly formation by the interaction of a magnetic discontinuity with the bow shock, *J. Geophys. Res.*, *98*, 15,319–15,330.

Winterhalter, D., M. G. Kivelson, C. T. Russell, and E. J. Smith (1981), ISEE-1, -2 and -3 observation of the interaction between an interplanetary shock and the Earth's magnetosphere: A rapid traversal of the magnetopause, *Geophys. Res. Lett.*, *8*, 911–914.

V. Angelopoulos, IGPP, ESS, University of California, Box 951567, Los Angeles, CA 90095, USA.

J. P. Eastwood, D. Larson, J. P. McFadden, and T. D. Phan, Space Sciences Laboratory, University of California, 7 Gauss Way, Berkeley, CA 94720-7450, USA.

M. J. Engebretson, Department of Physics, Augsburg College, Minneapolis, Minnesota, USA.

K.-H. Fornaçon, IGEP, Technische Universität Braunschweig, D-38106 Braunschweig, Germany.

K. S. Jacobsen and J. I. Moen, Department of Physics, University of Oslo, Postbox 1048, Blindern, N-0316 Oslo, Norway. (knutsj@fys.uio.no)

G. Provan, Department of Physics and Astronomy, University of Leicester, University Road, Leicester LE1 7RH, UK.

D. G. Sibeck, NASA Goddard Space Flight Center, Code 674, Greenbelt, MD 20771, USA.